

Recirculating induction accelerators as drivers for heavy ion fusion*

J. J. Barnard,[†] F. Deadrick, A. Friedman, D. P. Grote, L. V. Griffith, H. C. Kirbie, V. K. Neil, M. A. Newton, A. C. Paul, W. M. Sharp, and H. D. Shay
Lawrence Livermore National Laboratory, Livermore, California 94550

R. O. Bangerter, A. Faltens, C. G. Fong, D. L. Judd, E. P. Lee, L. L. Reginato, and S. S. Yu
Lawrence Berkeley Laboratory, Berkeley, California 94720

T. F. Godlove
FM Technologies, Inc., 10529-B Braddock Rd., Fairfax, Virginia 22302

(Received 7 December 1992; accepted 4 March 1993)

A two-year study of recirculating induction heavy ion accelerators as low-cost driver for inertial-fusion energy applications was recently completed. The projected cost of a 4 MJ accelerator was estimated to be about \$500 M (million) and the efficiency was estimated to be 35%. The principal technology issues include energy recovery of the ramped dipole magnets, which is achieved through use of ringing inductive/capacitive circuits, and high repetition rates of the induction cell pulsed, which is accomplished through arrays of field effect transistor (FET) switches. Principal physics issues identified include minimization of particle loss from interactions with the background gas, and more demanding emittance growth and centroid control requirements associated with the propagation of space-charge-dominated beams around bends and over large path lengths. In addition, instabilities such as the longitudinal resistive instability, beam-breakup instability and betatron-orbit instability were found to be controllable with careful design.

I. INTRODUCTION

Heavy ion fusion (HIF) has been identified by recent advisory studies^{1,2} as the leading candidate for an inertial fusion energy (IFE) power plant driver. Some advantages of HIF include the high efficiency and high repetition rate inherent to particle accelerators, the use of a magnetic lens in the final focus, assuring its survivability, and favorable target illumination geometry arising from the small solid angle subtended by the beams at the target. The induction accelerator is the leading U.S. candidate for HIF. Induction accelerators can inherently transport more current than radio-frequency (rf) accelerators, and systems studies suggest favorable costs for induction linac drivers.

In this paper we present some of the major results of a two-year study of recirculating induction accelerators (referred to here as recirculators). The potential for cost reduction motivated the study. The goals of the study were to produce a few design examples of recirculators, from which concrete cost and efficiency estimates could be determined. In addition, the designs allowed us to determine some of the major physics and engineering issues of the recirculator. The complete recirculator report may be found in Ref. 3.

Recirculators are circular induction accelerators which reuse their components up to 100 times for each beam pulse, thus requiring fewer components and hence offering the possibility of a large savings in cost. The length of a linear induction accelerator is determined by the maximum average accelerating gradient achievable, which is about 1

MV/m. For a 10 GeV heavy ion this results in a length of 10 km/ q where q is the charge state of the ion. In contrast, the circumference of the recirculator is determined by the bending radius of a 10 GeV ion in an average bending magnetic field of about 1 T. This suggests a minimum ring circumference of about 1.3 km/ q for the highest energy ions (with atomic mass 200). Since the components are used repeatedly the accelerating gradient may be reduced by an order of magnitude. This reduced gradient results in induction cores which are smaller than those of a linear accelerator. The combination of smaller cores and fewer components has a major impact on reducing the driver cost. However, ramped magnetic dipoles, increased induction core pulsed repetition rates, and longer path lengths traversed by the beam are all more demanding in the recirculator and therefore the impact of these issues on the design must be considered, and are the subject of this paper.

In Sec. II, we present an overview of one of our recirculator designs. In addition, we outline some of the considerations which led to the conceptual design of the three major systems of the accelerator: the acceleration modules, the bending magnets, and the focusing magnets. In Sec. III, the results of our cost and efficiency estimates are given, confirming our initial belief that a cost reduction is possible. Surprisingly, despite the introduction of energy losses in the dipole magnets, the overall efficiency of the recirculator was found to be at least as large as a comparable linear accelerator. In Secs. IV and V, the major engineering and physics issues are addressed, and we summarize our results in Sec. VI.

*Paper 2I3, Bull. Am. Phys. Soc. 37, 1379 (1992).

[†]Invited speaker.

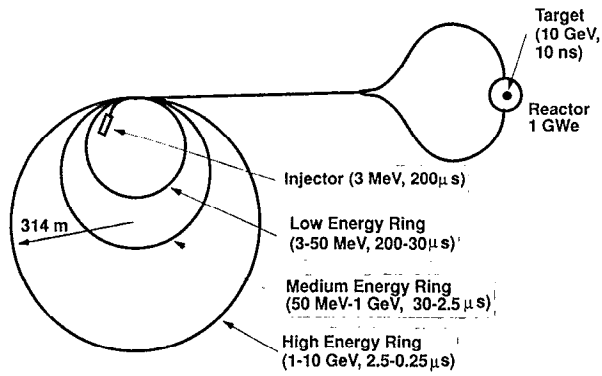


FIG. 1. Schematic layout of a recirculating induction accelerator.

II. RECIRCULATOR DESIGN CONSIDERATIONS

For the purpose of the report, we adopted a number of parameters which were primarily dictated by target and reactor physics and power plant economics. An end-to-end optimization including target and reactor chamber considerations may well yield a somewhat different set of requirements.

We adopted 200 as the atomic mass of the heavy ion, which, together with a stopping range of 0.15 g cm^{-2} , gives a required heavy ion energy of 10 GeV .⁴ By choosing the largest ion mass, we maximize allowed ion energy (for a given stopping range) and thus minimize the current. For a charge state of $+1$ and a required pulse energy of 4 MJ this translates into a total beam charge of $400 \mu\text{C}$.

At a range of 0.15 g cm^{-2} , a spot radius r_{spot} of 2 mm , and a pulse energy W of 4 MJ , the Lawrence Livermore National Laboratory gain curves for indirectly driven targets yield a gain of approximately 57 and a required peak power level of approximately 350 TW . These parameters imply a pulse length of approximately 11 nsec . The fusion energy per burst would be 230 MJ . Assuming a thermal efficiency ϵ of 41% , a blanket multiplication factor M of 1.15 , a repetition rate of 10 Hz , and an accelerator efficiency η of 35% yields a net electric power $P_e = v_{\text{rep}} W (\epsilon M G - 1/\eta) \approx 1 \text{ GW}$.

Figure 1 schematically depicts the recirculator layout. The injection energy is 3 MeV . Upon exit from the injector, the beam passes through three rings making 100 laps through each ring. Three rings were chosen, in order to restrict the dynamic range in energy in each ring to about 20. There are four beam lines throughout, and at each longitudinal position the beam lines pass through a single induction core. Pulse compression occurs continuously throughout the three rings. On exit from the high-energy ring (HER) the tails of the beams receive an additional velocity increase relative to the heads (i.e., "velocity tilts") in a linear bunching section, and drift compress to the target reaching their final pulse duration as they hit the target. A summary of some of the characteristics of the rings is presented in Table I.

Each ring consists of a number of lattice elements, arranged in a large circle, interrupted only by the linear

TABLE I. Summary of ring parameters.

	LER	MER	HER
Ion energy (GeV)	0.003–0.05	0.05–1	1–10
Pulse duration (μsec)	200–30	30–2.5	2.5–0.25
Circumference (m)	700	921	1976
Current/beam (A)	0.5–3.3	3.3–40.0	40.0–400.0
No. of beams	4	4	4
No. of core lines	1	1	1
No. of laps	100	100	100
Pipe radius (m)	0.078	0.064	0.061
Lattice half-period (m)	0.85	1.56	3.51
Induction modules:			
Inner radius (m)	0.313	0.255	0.243
Outer radius (m)	0.455	0.554	0.363
Length (m)	0.403	0.837	0.895
No. of cores	785	551	1068
Cell voltage (kV)	0.60	17.4	85
Bends (ramped magnetic dipoles):			
Effective length (m)	0.15	0.41	1.15
No. of Bends	2680	1796	1919
Max. B field (T)	0.90	0.85	0.81
Superconducting magnetic quadrupoles/dipoles:			
Length (effective length) (m)	0.47 (0.23)	0.92 (0.73)	1.94 (1.76)
No. of quads	3139	2201	2133
Quadrupole B field (T)	2.0	1.25	1.0
Dipole B field (T)		0.75	1.01
Max. total bending field (T)	0.16	0.58	0.77
(Averaged over lattice period)			

injection/extraction/transition sections. The lattice arrays consist of induction modules for acceleration, dipole magnets for bending the beam, and quadrupole magnets for focusing the beam. Additional space is allotted for vacuum, control, and diagnostics.

The induction cores are composed of annular cylinders of ferromagnetic material enclosed by a conducting shell to which a voltage pulse is applied. The changing magnetic flux induces an electric field which appears across the acceleration gap. Each core provides a voltage increment V_c for a duration τ satisfying

$$V_c \tau = \Delta B A_c, \quad (1)$$

where ΔB is the magnetic flux swing in the ferromagnetic material and $A_c = (R_o - R_i) L_c$, R_i and R_o being the inner and outer radii of the core material and L_c the length of the core. The ferromagnetic material we have chosen for cost and efficiency considerations is METGLAS⁵ 2605-S2. The maximum flux swing in this material before saturation is approximately 2.9 T . Because of the low-voltage gradient in the recirculator, the voltage on each cell can be reduced from that of a linear accelerator. Equation (1) indicates that the low voltages allow pulse durations to be made longer and/or core cross sections to be reduced. Longer pulse durations are utilized in the low-energy ring and permit the transport of $400 \mu\text{C}$ of charge in only four beams. Smaller cores in the HER provide cost savings.

Two types of dipole bending magnets are used: time-independent superconducting (for high efficiency) and

temporally ramped (to accommodate the increasing energy of the beam). The magnetic rigidity $[B\rho]$ of a heavy ion is given by

$$[B\rho] = \gamma A m_d \beta c / qe. \quad (2)$$

Here q is again the heavy ion charge state, γ is the Lorentz factor of the heavy ion, β is the heavy ion velocity in units of c , A is the atomic weight of the heavy ion, and e is the proton charge. The recirculator circumference C is then given by

$$C = 2\pi [B\rho]_{\max} / \eta_d B_d. \quad (3)$$

Here, $[B\rho]_{\max}$ is the rigidity at maximum energy achieved in a ring. The quantity $\eta_d B_d$ is the product of the dipole magnetic field and effective length of the dipole divided by the lattice half-period, summed over the time-independent field component and maximum of the temporally ramped component. For a fixed ratio of ramped to superconducting dipole field, the energy stored in the field is linear in B_d because the energy density is proportional to B_d^2 but the volume of field energy is proportional to C and hence to $1/B_d$. Since the dipole energy losses are approximately proportional to the total ramped field energy, the dipole losses are roughly proportional to $1/C$, favoring larger rings. On the other hand, use of the superconducting component allows us to design a relatively small ring (and thus reduce costs) without substantially sacrificing efficiency.

The superconducting quadrupoles comprise the third major element in a lattice period. In our conceptual design the superconducting quadrupoles and dipoles are combined into a combined function magnet, so that the occupancy factor (i.e., the effective length of the magnet divided by the lattice half-period) is the same for both. One could also place them sequentially with half the occupancy and twice the field strength with minimal effects on the design. The quadrupoles are placed within the induction cores to reduce the overall circumference of the recirculator. The requirements on the quadrupoles can be illustrated by the use of the "envelope" equation in the "smooth approximation," in which an average over a complete lattice period is used in calculating the focusing strength. A more complete treatment⁶ which includes the effects of the finite length of the magnetic quadrupoles is included in Ref. 3;

$$\frac{d^2 a}{dz^2} \cong -\frac{\sigma_0^2 a}{4L^2} + \frac{K}{a} + \frac{\epsilon_N^2}{\gamma^2 \beta^2 a^3}. \quad (4)$$

Here, a is the average beam radius, σ_0 is the phase advance per lattice period. The phase advance refers to the phase of harmonic oscillation the beam centroid experiences in one lattice period, arising from the focusing field of the quadrupoles. (In contrast, the depressed phase advance σ refers to the phase of harmonic oscillation a single particle experiences, due to the effective restoring force, which is a combination of the outward space-charge force of the beam and the inward focusing force of the quadrupoles.)

The generalized perveance $K = 2qI_b / (I_0 \gamma^3 \beta^3 A)$ is a dimensionless measure of the current relative to energy, I_b is the current in each beam, $I_0 = 4\pi\epsilon_0 m_d c^3 / e = 31$ MA, ϵ_0 is

TABLE II. Summary of major cost assumptions.

Item	Unit cost
METGLAS ⁵ in the induction cores	\$5/kg
Peak pulse power (per induction cell)	\$0.12/kW
Insulator material	\$122/kg
Magnetic dipole pulsers	\$0.20/J
Superconductor material (NbTi)	\$300/kg
Copper in superconductors	\$50/kg
Iron in ramped dipoles	\$20/kg
Quadrupole power supplies	\$0.003/J
Vacuum pumps	\$5/1/sec

the free-space permittivity, and ϵ_N is the normalized emittance which is a measure of the transverse phase space occupied by the beam. The phase advance per period is given approximately as

$$\sigma_0 \cong \eta_q B' L^2 / [B\rho], \quad (5)$$

where B' is the magnetic field gradient in the quadrupole ($\cong B/r_p$), η_q is the occupancy fraction of the quadrupole, and r_p is the pipe radius.

The beam current increases as the velocity increases and the pulse duration decreases, causing the average beam radius to increase slightly in each ring. In Eq. (4), the first term on the right-hand side (arising from the focusing quadrupoles) must balance the second term (due to the space charge of the beam) and to a lesser extent the third term (arising from the thermal forces). But there are constraints that limit the choices of r_p , L , B , B_d , η_q , and η_d .

Some of the constraints that led to the design are the requirement that the beam radius remain considerably less than the pipe radius, the requirement (for stability reasons) that the phase advance σ_0 remain less than 80° , and the requirement that the ratio of the lattice half-period to the pipe radius be greater than about 10 (to minimize nonlinearities in the focusing field). In addition, the often-conflicting requirements of low cost and high efficiency required several iterations to develop sensible example designs.

III. COST AND EFFICIENCY RESULTS

A systems code which used the design equations to determine the specifications of each component was developed. The total cost was the sum of component costs. That is, individual quadrupoles, dipoles, induction modules, etc., were designed and their costs determined on the basis of material quantities and assumed manufacturing costs. As parameters were changed the systems code calculated the amount of material required based on scaling of specific designs. Some of the cost assumptions that were used are listed in Table II. After all recirculator component costs were calculated, an allowance was made for some specific additional costs. Based on other accelerator projects, we assumed that administration, engineering, and installation each contributed an additional cost of 10% of the direct component costs. With these assumptions we arrived at a total cost of approximately \$500 M. The result is a signif-

icant reduction in cost from the conventional linac which was estimated in the Heavy Ion Fusion System Assessment studies⁷ to be about \$1000 M. However, other recent studies^{8,9} have suggested similar cost reductions, using a variety of cost saving techniques, including higher charge state, different material for superconductors, and multipulsing a linac into a set of storage rings. Present studies at Livermore in collaboration with W. J. Schafer Associates are in progress which are comparing linacs and recirculators using identical costing algorithms. In addition, both the linacs and recirculators are being optimized from injector to target, so that a fair comparison can be made between the two concepts.

In addition to estimating costs, the energy requirement of each component was calculated and a summation was made over all components. The energy budget was divided among three major elements: the beam consumed 35% of the supplied electrical energy, losses in the acceleration modules accounted for another 31%, and losses in the ramped dipole magnets accounted for another 24% of the energy. An additional 10% was lost in miscellaneous sources such as vacuum, refrigeration, and beam injection and extraction. The efficiency of 35% compared favorably to linear induction accelerators. This result is at first glance surprising since the addition of ramped dipole magnets provides energy consumption which does not occur in the linear machine. However, the lower voltage gradient allows smaller cores with lower individual voltages, making the induction cells much more efficient. In addition, the decomposition of the dipole field into an efficient time-independent component and a temporally ramped, energy-consuming component helped to minimize losses in the dipole magnets.

IV. ENGINEERING ISSUES

A number of engineering issues emerged as a result of the detailed specification of the design example. We shall focus on two key issues which are present in a recirculator but not present in a linear machine. The first issue is that of energy recovery of the ramped dipole field, and the second is the high repetition rates of the induction core pulsers.

As discussed in Sec. II, when the beam energy increases from lap to lap in each ring of the recirculator, the dipole field must ramp in time. In the high-energy ring for example, the total dipole field (averaged over a lattice period) changes from 0.24 T to a maximum of 0.77 T during the 3 msec that the beam is within the ring. As indicated in Sec. II, part of the field is produced by time-independent superconducting magnets, producing a field of 1.01 T with an occupancy of 0.5. The remainder of the field is produced by temporally ramped conventional magnets, which produce a field from -0.81 T to $+0.81$ T with an occupancy of 0.33. The maximum magnetic field energy stored in the ramped component is 48 MJ which is much larger than the 4 MJ beam energy. In order for the recirculator to be electrically efficient, a large fraction of that field energy must be recovered each pulse. One method of recovering the energy is to use the inductance of the ramped dipole magnet, together with storage capacitors to produce a ring-

ing LC circuit. In this scenario, energy is first stored in capacitors, switched to the magnetic field in the dipole magnets, and then recovered in the capacitors. The resulting magnetic field is then sinusoidal in time, and the beam circulates within the recirculator during the interval in which the field increases nearly linearly with time. Eddy current and hysteresis losses in the iron of the magnet, and eddy current and conductive losses in the copper conductors are the sources of energy loss in the ramped dipoles. In a one-quarter scale experiment at Livermore^{3,10} Reginato found a 90% recovery rate was possible, which was consistent with the energy loss calculations. For the parameters of the HER, we estimate that 94% energy recovery is possible. A second method also being considered uses alternating compulsators.¹¹ In this method, energy is stored in rotational energy of an alternator, and similar efficiencies should be produced in a reliable and cost effective way. In addition, the flexibility of producing a more triangularly shaped temporal profile (thus reducing the maximum required magnetic field) is also possible with alternating compulsators.

The second major engineering challenge for recirculators is the high repetition rates of the induction modules. As the energy of the beam increases in each ring the orbital time decreases and so the repetition rate of the induction cells increases from 15 to 50 kHz in the high-energy ring. In addition, pulse compression occurs during acceleration, so the pulse duration must decrease from 2.5 to 0.25 μ sec. Field effect transistors (FET's) were chosen to act as opening and closing switches to deliver power to the induction cells. FET technology has already been developed for some high-voltage applications, although not to the scale required for the recirculator nor at the desired cost. An integrated induction core and modulator is being developed at Lawrence Livermore National Laboratory (LLNL) using FET switches to deliver the accelerating voltage pulse to the induction cells.¹² The near-term objective of this work is to develop a modulator capable of delivering 5 kV, 1–2 μ sec pulses at 200 kHz to a METGLAS⁵ induction cell, suitable for a small-scale (100 m) recirculator. To date, a two-by-two array of switches in series and parallel has been tested at 1 kV and 200 kHz. The repetition rate achieved in the experiment exceeds the requirements for all three rings of the driver recirculator. One uncertainty is the cost of the switches. Our assumption of \$0.12 per kW of peak power is a factor of 4 reduction from the current price of the IRF 840 MOSFET. Ten to fifteen years ago the cost of this switch was 12.5 times larger than the current price, so we believe that our estimate of a factor of 4 decrease over the next 20 to 30 years is not an unreasonable one.

V. PHYSICS ISSUES

In an HIF power plant, high beam quality must be maintained throughout the accelerator in order to focus the beam onto a sufficiently small spot at the target.¹³ Here beam quality refers to the combination of high current and low normalized emittance. There are a number of processes which degrade the beam quality, by either increasing the

transverse or longitudinal emittance, or by removing particles from the beam. In this section, we focus on those processes which degrade beam quality and are more demanding in a recirculator than in a linear induction accelerator. The total path length traversed by a beam pulse is about 360 km from injector to target. This is about 36 times longer than in an equivalent linear accelerator. Many of the issues which are more demanding in a recirculator are a result of this longer path length. Among these issues are higher vacuum requirements and more demanding control of centroid position and transverse emittance. In addition, attention must be paid to the control of transverse instabilities, in order to ensure that the beam does not hit the wall and the transverse emittance does not grow. Longitudinal instabilities must also be controlled, so that uncontrolled beam bunching and growth of the longitudinal velocity spread do not occur.

Particle loss can occur through collisions with background gas particles and other heavy ions. Our criterion for allowable loss was simply that the current at the target meet the current goal of 100 kA. Our procedure was to produce a design which was assumed at first to have zero beam loss. The loss from the then calculable beam density was then known. This required adding more charge to the beam at the injector, which altered the recirculator design requiring, for example, longer pulse durations to account for the additional space charge. Since we worked in a regime where only a few percent of the beam was lost per ring, the procedure quickly converged.

A number of processes which cause loss of particles from the heavy ion beam have been identified.¹⁴⁻¹⁷ The processes which we considered are beam-beam charge exchange, stripping, background gas ionization, and beam-induced gas desorption. Beam-beam charge exchange occurs when two of the beam ions interact, transferring an electron from one ion to the other. The result is a neutralized ion and a doubly charged ion. Both particles will hit the beam-pipe wall in a distance that is small compared to the circumference of the recirculator. The particle density and transverse velocity determine the reaction rate. The fractional beam loss $\delta n_b/n_b$ from beam-beam charge exchange is approximately given by

$$\frac{\delta n_b}{n_b} \cong 0.02 \left(\frac{A}{200} \right)^{0.62} \left(\frac{\epsilon_N}{6.3 \times 10^{-6} \pi \text{ mrad}} \right)^{2.24} \left(\frac{Q_b}{100 \mu\text{C}} \right) \times \left(\frac{6.1 \text{ cm}}{r_p} \right)^{4.24} \left(\frac{0.46}{\eta_p} \right)^{4.24} \left(\frac{37 \text{ m}}{l_b} \right) \left(\frac{\Delta t}{3.2 \text{ msec}} \right). \quad (6)$$

Here we have assumed the cross section for a heavy ion to change charge states due to an interaction with another heavy ion $\sigma_{ce} \cong 2.1 \times 10^{-16} (E_{cm}/10 \text{ keV})^{0.62} \text{ cm}^2$ (see Refs. 18 and 19). Also, n_b is the ion-beam number density; A is the heavy ion atomic mass; ϵ_N is the normalized emittance; $E_{cm} = Am_u v_{cm}^2/2$; $v_{cm} \cong \epsilon_N c/a$; Q_b is the charge in each ion bunch, the beam radius a is a fraction η_p of the pipe radius r_p , l_b is the bunch length, and Δt is the residence time of the bunch within the recirculator. Note the steep dependence of the charge exchange loss on the pipe radius. Here large pipe radii permit large radius beams (and thus lower

beam density) and smaller transverse velocities (with smaller cross section and smaller collision rate).

Stripping occurs when an electron is stripped from a heavy ion through an interaction with a residual gas molecule, and the ion is again lost from the beam. The maximum background gas density can be determined by consideration of the mass continuity equation of the heavy ion beam, which approximately yields,

$$n_g \cong \frac{(\delta n_b/n_b)_{\text{strip}}}{\sigma_s n_{\text{lap}} C}. \quad (7)$$

Here $(\delta n_b/n_b)_{\text{strip}}$ is the fractional beam loss due to stripping, σ_s is the cross section for a background gas molecule to strip an electron off of a heavy ion, n_{lap} is the number of laps of the recirculator of circumference C , satisfying $n_{\text{lap}} C \cong v_i \Delta t$, where v_i is the heavy ion velocity. Equation (7) simply indicates the scaling that the required gas density is inversely proportional to the total path length traversed by the beam.

Background gas ionization occurs when a beam ion strips an electron off of a neutral residual gas molecule. Background gas ionization does not lead to beam loss directly, but rather indirectly through interactions with the walls. Beam-induced gas desorption occurs when an ionized background gas molecule, accelerated by the space charge of the beam, hits the wall, emitting η_G gas molecules. The background molecule hits the wall at an energy which is typically tens of keV. The desorption coefficient is of order a few; we take $\eta_G \cong 5$. In addition, when doubly ionized or neutral heavy ions hit the wall they will desorb η_{HI} gas molecules.

By consideration of the continuity and momentum equations of the background gas the total pumping rate may be obtained (as done in Refs. 3 and 20 and references therein):

$$S_{\text{lin}} C \cong N_b n_{\text{lap}} C \left(\frac{\sigma_s Q_0 A_{sp}}{(\delta n_b/n_b)_{\text{strip}}} + \frac{([\eta_G - 1] \sigma_i + \eta_{\text{HI}} \sigma_s) Q_b}{qe t_r} \right). \quad (8)$$

Here S_{lin} is the average pump rate per unit distance along the accelerator, Q_0 is the intrinsic gas desorption rate per unit area, N_b is the number of beams; η_G is the number of molecules desorbed from the pipe inner wall per incident gas molecule; η_{HI} is the number of molecules desorbed from the pipe inner wall per incident heavy ion; qe is the ion charge; t_r is the repetition time for pulses in the recirculator, and $A_{sp} = 2\pi r_p C$ is the total surface area of a single beam pipe. Equation (8) is approximately true when appropriate averages are made over cross sections and desorption coefficients and also when the beam-induced wall desorption is not undergoing an exponential growth. Equation (8) simply equates the rate at which the total number of gas particles are removed from the recirculator [proportional to the left-hand side (lhs)] to the time-averaged rate at which the gas particles are produced [proportional to the right-hand side (rhs)]. The first term on the rhs is proportional to the intrinsic outgassing (and therefore pro-

portional to the pipe radius) and the second term on the rhs is from induced outgassing. Here each stripped ion is assumed to produce η_{HI} molecules upon hitting the wall and each ionized gas molecule produces η_G gas molecules upon hitting the wall. Equation (8) assumes that the induced outgassing is small enough so that the gas pressure is increasing linearly with time during the time the beam is within the recirculator. For large enough desorption rates, however, the gas will increase exponentially. The condition for one e -fold of growth of the background gas can be expressed as a condition on r_p as

$$r_p > \sim \left(\frac{([\eta_G - 1]\sigma_i + \eta_{HI}\sigma_s)Q_b n_{lap}}{\pi q e} \right)^{1/2}. \quad (9)$$

From Eqs. (8) and (9) we can see that the total pumping rate decreases as r_p decreases (as the intrinsic gas desorption decreases) but then increases with further decrease of the pipe radius as the beam-induced desorption becomes significant. As an example, in the high-energy ring, $N_b=4$, $n_{lap}=100$, $C=2.0 \times 10^3$ m, $Q_0 \sim 10^{-11}$ Torr $l \text{ sec}^{-1} \text{ cm}^{-2}$, $(\delta n_b/n_b)_{strip}=0.015$, $\eta_G \sim 5$, $\sigma_i \sim 5 \times 10^{-16} \text{ cm}^2$, $\eta_{HI} \sim 0.01$, $\sigma_s \sim 6 \times 10^{-17} \text{ cm}^2$, $Q_b=100 \mu\text{C}$, $q e=1.6 \times 10^{-19} \text{ C}$, $t_r=0.1 \text{ sec}$, so that $S_{lin}C=2.4 \times 10^6 l \text{ sec}^{-1}$, which translates into a pumping cost of \$12 M assuming a unit cost of \$5 $l^{-1} \text{ sec}$. The required background gas density would then be about 2×10^{-10} Torr. The critical pipe radius from Eq. (9) is about 7 cm indicating that the gas increases by about an e -fold during the residence time of the beam, but is pumped back down to the initial density during the 0.1 sec interval between pulses. Note that Eqs. (8) and (9) do not include charge-exchange-induced desorption, and are meant to illustrate scaling on some of the recirculator parameters. A more exact calculation of the vacuum requirements can be found in Ref. 3.

Large uncertainties exist in our knowledge of η_G and particularly η_{HI} . Extrapolation of sputtering coefficients at low energy to high energy would suggest that η_{HI} should be less than unity, and the dominant contribution to desorption would then come from ionization. Some data and theory,^{21,22} however, suggest that η_{HI} is of order 5 for some coarse grain metals, and can be much larger (~ 1000) for fine grained metallic films. In our design, we made the optimistic assumption that beam desorption from ionized background gases made the dominant contribution to beam-induced desorption ($\eta_G \gg 5 \gg \eta_{HI} < 1$). For values of η_{HI} as high as 5, the vacuum system would increase in cost by $\sim 65\%$, but would still be a relatively small fraction of the total cost. For values of η_{HI} as high as 1000, substantial reoptimization of the recirculator would be required. Measurement of η_{HI} in the appropriate energy range and with appropriate materials is vitally important for a reliable recirculator design.

The second major physics issue which is more demanding in a recirculator is beam centroid control. A beam whose centroid is off-axis will oscillate harmonically in the focusing channel. These oscillations are known as betatron oscillations. Misalignments of quadrupoles result in a cen-

triod betatron amplitude x_c which increases like a random walk, giving

$$x_c^2 \cong C_{rw} N_q \delta x_{rms}^2. \quad (10)$$

Here, N_q is the number of quadrupoles with rms displacement δx_{rms} through which the beam passes; C_{rw} has been determined by detailed numerical calculations³ and has been shown to vary from about 6 to 3 in the HER. The longitudinal distance traveled by the beam $z=N_q L$, where L is the half-period lattice (3.5 m in the HER). In addition to quadrupole misalignments dipole magnetic field errors also contribute to the random walk off axis. For a path length of 200 km in the HER, and a maximum beam displacement of 1 mm, this analysis gives a quadrupole alignment requirement of about 10μ and a dipole field error tolerance of less than one part in 5×10^4 . These alignment criteria are stringent but not impossible. However, the criteria are considerably relaxed when steering stations are included in the design. If δx_{rms} is 100μ and the allowed beam displacement is about 1 mm, then impulses steering the beam to $x_c=x'_c \cong 0$ must occur at an interval along the accelerator of $L x_c^2 / (C_{rw} \delta x_{rms}^2)$, which is about $16.7L$ for the above parameters. A betatron period is $(4\pi/\sigma_0)L$ which has a minimum value of about $9L$, implying a correction would be required once every two betatron periods. Since the circumference is about 2 km, there would be about 34 such steering sections in the HER. When the beam has reached its final energy in the HER, C_{rw} is reduced by a factor of 2 from its initial value, so x_c will be reduced to about 0.7 mm. Conceptually, the steering stations would consist of three monitors, to infer the position and transverse velocity of the centroid, as well as the beam energy on a given lap of the acceleration sequence. In addition to the monitors a pair of dipole magnets with adjustable field strengths ("dipole kickers") would be used to first zero the centroid displacement from the design orbit and then, second, to zero the transverse velocity. These kicks would be constant over the duration of the pulse. In addition, one time-dependent kicker station per ring would be required to prevent phase differences from accumulating between the beam center and the ends. Simulations using the code CIRCE (a transverse envelope-longitudinal Lagrangian fluid code²³) are being used to develop optimized steering algorithms.

In addition to centroid control, emittance growth must be minimized. The normalized emittance is a measure of the transverse phase space occupied by the beam and is an invariant in an ideal focusing system. In order to focus onto a spot at the target, the normalized emittance cannot be too large. We estimate that, from injector to target, a growth in normalized emittance by a factor of order 20 is allowable. Two sources of emittance growth have been identified. The first is conversion of centroid oscillation energy into thermal energy; the second is the conversion of transition mismatch oscillation energy into thermal energy.

As discussed above, centroid misalignments give rise to betatron oscillations. In the presence of nonlinearities in the focusing fields, some of the transverse energy associated with oscillation of the beam centroid is converted into

thermal energy. Using the approximations of smooth focusing, constant velocity, and total conversion of centroid transverse energy into thermal energy^{3,24} implies that the increased normalized emittance $\Delta\epsilon_N$ can be approximately written:

$$\Delta\epsilon_N \cong \beta C_{rv} \frac{\sigma_0^2 \delta x_{rms}^2}{\sigma L^2} n_{lap} C. \quad (11)$$

Here, using typical numbers from the high-energy ring, $(\beta C_{rv} \sigma_0^2 / \sigma) \cong 1.3$, lattice half-period $L = 3.5$ m, the number of laps the beam makes in the ring $n_{lap} = 100$, the circumference $C = 2.0 \times 10^3$ m, we find a $\Delta\epsilon_N \cong 2.0 \times 10^{-6} \pi$ mrad if the rms alignment error $\delta x_{rms} = 10 \mu$. This compares to a final normalized emittance of about 7.5×10^{-6} mrad in the design for the high-energy ring. Steering will increase the tolerance on emittance growth by a factor $(L_{pm}/L_s)^{1/2}$ where L_{pm} is the phase mixing distance and L_s is the distance between steering stations. A factor of 10 increase in the alignment tolerance would be a reasonable expectation (yielding a tolerance of $\sim 100 \mu$). We emphasize that this is a pessimistic estimate based on the assumption that all centroid oscillation energy is converted into emittance growth.

The second source of emittance growth was first observed in 3-D particle-in-cell simulations using the code WARP.^{25,26} For a beam which is in equilibrium in a straight section and then enters a bend, the beam becomes mismatched for the bend. Physically, particles that are not on the design momentum for the bend initially become spatially separated, creating nonlinear space-charge forces, allowing phase mixing of the coherent mismatch oscillations, until a new equilibrium is reached. The simulations showed that if a beam enters a bend from a straight section the emittance initially grows but saturates in a few betatron periods, as a new equilibrium is approached. However, in a racetrack configuration composed of 180° bends separated by linear sections the emittance continues to grow, since new mismatches are formed at each transition. The simulations were done for a small-scale recirculator, similar to one that is being proposed as an experiment in the Induction Linac Systems Experiments, now being planned at Lawrence Berkeley Laboratory. A linear theory²⁷ was developed in which beam displacement and particle energy spread were both treated as linear quantities. Transverse energy conservation was assumed, as well as complete conversion of mismatch energy into thermal energy. For large energy spreads and highly tune-depressed beams the theory tracked the simulations closely, with theory overestimating the emittance growth when the assumption of complete conversion of mismatch energy was violated. When the parameters of the beam at the exit of the high-energy ring are used, the theory predicts a factor of 2 increase in emittance, within the allowed emittance budget. It is conjectured that the transitions may be made gradual enough so that equilibria are reached adiabatically with even less growth in the normalized emittance.

The final physics issues addressed here involve beam instabilities. Three instabilities are discussed: the longitu-

dinal resistive instability, the transverse beam-breakup instability, and resonance instability.

A major research effort on the subject of the longitudinal resistive instability in HIF induction accelerators has been made over the last few years (cf. Ref. 28 and references therein). In this instability, the beam can become bunched due to the impedance of the induction cavities. However, recent studies show that the growth rates and instability gains that were obtained in the early 1980s overestimated the instability gain since they neglected the capacitance of the induction modules. Also, feed-forward techniques can be utilized to further control residual growth. In the recirculator the voltage gradient is reduced from that of the linear machine. For line-type modulators, the impedance of the line must be matched (or nearly matched) to the impedance of the load, which is nearly proportional to the cell voltage divided by the total current. Thus, with a small voltage gradient (for a given current) the resistance is reduced. When opening and closing switches are used to modulate the voltage pulse to the induction cores the matched condition is not necessary and the cell resistance may be reduced further. For these reasons, we find that the instability should be less severe in a recirculator, and that the solutions found in Ref. 28 may also be used for residual growth of the instability.

The second instability known to occur in induction linacs is the beam-breakup instability. In this instability, displacements in the head of the beam excite electromagnetic modes in the cavities formed by the acceleration gaps of the induction cells. The fields that are excited give kicks to the rest of the beam, causing displacements, and more excitation and so forth. In the recirculator (and linear driver) strong focusing (alternating gradient) is used, in contrast to the weaker solenoidal focusing used in many electron induction linacs. In addition, at the lower energies, the beam takes a relatively long time to transit the gap so that the electric field oscillates in time, averaging out to give a small net kick. The gain of the instability in the HER is estimated to be unity, provided that the cells can be designed such that the Q of the cavity can be reduced to be of order a few. Cell designs using the electromagnetic field code AMOS²⁹ or the 3-D version PLATO should make such low values of Q possible.

The final instability which is often brought up in the context of circular machines is the resonance instability. In a storage ring, the orbital period cannot be an integral number of betatron periods. Otherwise a misalignment would give the beam a kick at the same phase of its betatron oscillation. This would lead to a larger and larger centroid displacement, and would ultimately result in the beam hitting the wall. In a recirculator, however, the focusing field remains constant while the beam accelerates. The betatron period thus increases as the energy increases. In the HER the number of betatron periods varies from 63 to 20 in 100 laps. The betatron phase changes by an average of 140° per lap, and therefore the kicks given by the misalignments add more randomly than coherently. The machine behaves like a long linear accelerator and the dis-

discussion about misalignments in the section above on centroid control becomes pertinent.

VI. CONCLUSIONS

We have shown that, using our best estimates of physical parameters and component costs, a 4 MJ recirculator driver, with an efficiency of 35% would have a projected cost of approximately \$500 M. The cost and efficiency compares favorably with previous estimates of these quantities for linear induction accelerators. Studies are currently underway, however, to compare recirculators with linear induction machines using identical costing algorithms. Crucial engineering issues which we have identified include the high repetition rates of the induction core pulsers, and efficient energy recovery in the ramped dipole magnets. Small-scale experiments are in progress to validate the engineering solutions to these issues. In addition, a recirculator ring is being planned for the proposed Induction Linac Systems Experiments facility, currently being designed at the Lawrence Berkeley Laboratory. This ring would provide an integrated test of the recirculator concept. Crucial physics issues include the maintenance of the high vacuum, beam centroid, and beam emittance control, as well as control of longitudinal and beam breakup instabilities. Our studies to date have not revealed insurmountable hurdles, although critical desorption coefficient data are required to validate our assumptions concerning the vacuum system. In general, we find that a driver based on the induction recirculator is an economically attractive candidate for an HIF power plant and that it merits further experimental and theoretical research.

ACKNOWLEDGMENTS

In addition to the authors of this paper many people contributed to our recirculator studies. Some of these people include W. A. Barletta, A. L. Brooks, R. Bieri, D. Callahan, J. P. Clay, F. Coffield, J. DeFord, W. M. Fawley, T. J. Fessenden, W. L. Gagnon, A. R. Harvey, J. R. Heim, D. W. Hewett, D. C. Ho, W. J. Hogan, C. A. Hurley, A. B. Langdon, E. J. Lauer, J. L. Miller, R. W. Moir, H. G. Patton, G. E. Russell, C. Shang, S. Shen, D. S. Slack, and L. Smith.

Work performed under the auspices of the U.S. Department of Energy at Lawrence Livermore National Laboratory under Contract No. W-7405-ENG-48 and at Lawrence Berkeley Laboratory under Contract No. DE-AC03-76SF00098.

APPENDIX: TABLE OF SYMBOL DEFINITIONS

a :	average beam radius;
A :	heavy ion mass in atomic mass units;
A_c :	$=I_c(R_o - R_i)$ = the cross-sectional area of the METGLAS ⁵ core;
A_{sp} :	$=2\pi r_p L_{rec}$ = total surface area of one beam pipe;
B :	quadrupole magnetic field at the pipe radius;
B_d :	dipole magnetic field within pipe;
$[B\rho]$:	magnetic rigidity;

$[B\rho]_{max}$:	magnetic rigidity at the maximum ion energy in a particular recirculator ring;
B' :	$=B/r_p$ = transverse magnetic gradient in quadrupole;
c :	speed of light;
C :	recirculator circumference;
C_{rw} :	numerically derived constant, ratio of mean square centroid position to $N_q \delta x_{rms}$;
e :	magnitude of the electron charge;
G :	target gain;
I_b :	current per beam;
I_0 :	$=4\pi\epsilon_0 m_u c^3 / e = 31$ MA;
K :	$=[2q/(\gamma^3 \beta^3 A)](I_b/I_0)$ = the generalized permeance;
l_b :	bunch length;
L :	lattice half-period;
L_c :	length of METGLAS ⁵ core;
L_{pm} :	distance for nonlinearities to phase mix betatron oscillations;
L_s :	distance between steering modules;
m_u :	atomic mass unit;
M :	blanket multiplication factor;
n_g :	mean background gas density;
n_{lap} :	number of laps the beam orbits a recirculator ring;
N_q :	number of quadrupoles transited by beam;
P_e :	net electric power;
q :	ion charge state in units of proton charge;
Q_b :	charge per beam;
Q_0 :	intrinsic outgassing rate per unit surface area of pipe;
R_i :	inner radius of METGLAS ⁵ core;
R_o :	outer radius of METGLAS ⁵ core;
r_p :	single pipe radius;
r_{spot} :	final spot radius on target;
S_{lin} :	pumping speed per unit distance from distributed pumps;
t_r :	repetition time between beam pulses;
v_{em} :	ion random velocity in the beam frame;
V_c :	voltage across an induction module;
W :	total pulse energy;
x_c :	beam centroid transverse position;
z :	path length along the accelerator;
β :	ion velocity in units of c ;
γ :	$= (1 - \beta^2)^{-1/2}$ = Lorentz factor of beam;
$\delta n_b/n_b$:	total fractional beam loss;
$(\delta n_b/n_b)_{ce}$:	fractional beam loss from charge exchange alone;
$(\delta n_b/n_b)_{strip}$:	fractional beam loss from stripping alone;
δx_{rms} :	root-mean-square quadrupole transverse error;
ΔB :	magnetic flux swing in induction material over pulse;
ϵ :	efficiency of conversion of thermal to electric energy;
ϵ_0 :	permittivity of free space $= 8.8542 \times 10^{-12}$ F/m;
ϵ_N :	normalized emittance;
η :	accelerator efficiency;

η_d :	dipole occupancy factor;
η_p :	ratio of average beam radius to pipe radius;
η_q :	quadrupole occupancy factor;
η_G :	wall desorption coefficient for ionized gas molecules;
η_{HI} :	wall desorption coefficient for heavy ions;
ν_{rep} :	repetition rate;
σ :	depressed phase advance;
σ_{ce} :	charge exchange cross section;
σ_i :	ionization cross section;
σ_0 :	undepressed phase advance per lattice period;
σ_s :	stripping cross section;
τ :	pulse duration.

¹Final Report Fusion Policy Advisory Committee (U.S. Department of Energy, Washington, DC, 1990), U.S. Department of Energy Report DOE/S0081.

²Review of the Department of Energy's Inertial Confinement Fusion Program Final Report, Committee for a Review of the Department of Energy's Inertial Confinement Fusion Program, National Academy of Sciences (National Academy Press, Washington, DC, 1990).

³See National Technical Information Service Document No. DE92016980. (J. J. Barnard *et al.*, "Study of Recirculating Induction Accelerators as Drivers for Heavy Ion Fusion," LLNL Report UCRL-LR-108095, September 1991.) Copies may be ordered from the National Technical Information Service, Springfield, Virginia 22161.

⁴D. Keefe, *Annu. Rev. Nucl. Part. Sci.* **32**, 391 (1982).

⁵METGLAS is a trademark for alloys of metal developed by Allied Signal, Inc., Parsippany, NJ.

⁶E. P. Lee, T. J. Fessenden, and L. J. Laslett, *IEEE Trans. Nucl. Sci.* **NS-26**, 2489 (1985).

⁷J. Hovingh, V. O. Brady, A. Faltens, D. Keefe, and E. P. Lee, *Fusion Technol.* **13**, 255 (1988).

⁸R. F. Bourque, W. R. Meier, and M. J. Monsler, *Fusion Technol.* **21**, 1465 (1992).

⁹L. M. Waganer, *14th IEEE/NPSS Symposium on Fusion Engineering*, October 1991 (Institute of Electrical and Electronic Engineers, New York, 1992).

¹⁰L. Reginato, M. Newton, and S. S. Yu, *Part. Accel.* **37-38**, 335 (1992).

¹¹W. F. Weldon, W. L. Bird, M. D. Driga, K. M. Tolck, H. G. Rylander, and H. H. Woodson, *Proceedings of the 2nd IEEE Pulsed Power Conference*, edited by A. H. Guenther and M. Kristiansen (Institute of Electrical and Electronic Engineers, New York, 1979), p. 76.

¹²See AIP document No. PAPS PFBPE-05-2698-5 for 5 pages of H. C. Kirbie, G. J. Caporaso, M. A. Newton, and S. S. Yu, *1992 Linear Accelerator Conference Proceedings*, 24–28 August 1992, Ottawa, Ontario, Canada, edited by C. R. Hoffman (Scientific Document Distribution Office, AECL, Chalk River, Ontario, Canada, 1992), Vol. 2, p. 595. Order by PAPS number and journal reference from American Institute of Physics, Physics Auxiliary Publication Service, 335 East 45th Street, New York, NY 10017. The price is \$1.50 for each microfiche (60 pages) or \$5.00 for photocopies of up to 30 pages, and \$0.15 for each additional

page over 30 pages. Airmail additional. Make checks payable to the American Institute of Physics.

¹³E. P. Lee, *Heavy Ion Inertial Fusion*, AIP Conf. Proc. 152, edited by M. Reiser, T. Godlove, and R. Bangerter (American Institute of Physics, New York, 1986), p. 461.

¹⁴See National Technical Information Service Document No. LBL-5543. (Y. K. Kim, Energy Research and Development Administration Summer Study of Heavy Ions for Inertial Fusion, LBL-5543, edited by R. Bangerter, W. Hermansfeldt, D. Judd, and L. Smith, Technical Information Division, Lawrence Berkeley Laboratory, Berkeley, CA, 1976, p. 11 and p. 58.) Copies may be ordered from the National Technical Information Service, Springfield, Virginia 22161.

¹⁵See National Technical Information Service Document No. LBL-5543. (G. H. Gillespie, Energy Research and Development Administration Summer Study of Heavy Ions for Inertial Fusion, LBL-5543, edited by R. Bangerter, W. Hermansfeldt, D. Judd, and L. Smith, Technical Information Division, Lawrence Berkeley Laboratory, Berkeley, CA, 1976, p. 59.) Copies may be ordered from the National Technical Information Service, Springfield, Virginia 22161.

¹⁶See National Technical Information Service Document No. BNL-50769. (D. Blechshmidt and H. J. Halama, Proceedings of the Heavy Ion Fusion Workshop, Brookhaven National Laboratory, October 17–21, 1977 BNL-50769, edited by L. W. Smith, Brookhaven National Laboratory Associated Universities, Inc., Upton, NY, 1977, p. 136.) Copies may be ordered from the National Technical Information Service, Springfield, Virginia 22161.

¹⁷See Ref. 16, p. 45.

¹⁸F. Melchert, E. Salzborn, I. Hofman, R. W. Muller, and V. P. Shevelko, *Nucl. Instrum. Methods Phys. Res. A* **278**, 65 (1989).

¹⁹E. Salzborn, *J. Phys. Coll. C1, Suppl.* **1**, 50 (1989).

²⁰J. J. Barnard, S. S. Yu, A. Faltens, *Part. Accel.* **37-38**, 419 (1992).

²¹I. A. Baranov, A. S. Krivokhatskii, and V. V. Obnorskii, *Zh. Tekh. Fiz.* **51**, 2457 (1981) [*Sov. Phys. Tech. Phys.* **26**, 1455 (1981)].

²²D. G. Koshkarev, *Part. Accel.* **16**, 1 (1984).

²³W. M. Sharp, J. J. Barnard, and S. S. Yu, *Part. Accel.* **37-38**, 205 (1992). Also, W. M. Sharp, J. J. Barnard, and S. S. Yu, in *Conference Record of the 1991 IEEE Particle Accelerator Conference*, San Francisco, edited by L. Lizama and J. Chew (Institute of Electrical and Electronic Engineers, New York, 1991), p. 260.

²⁴M. Reiser, *J. Appl. Phys.* **70**, 1919 (1991).

²⁵A. Friedman, D. P. Grote, D. A. Callahan, A. B. Langdon, and I. Haber, *Part. Accel.* **37-38**, 131 (1992).

²⁶A. Friedman, D. P. Grote, and I. Haber, *Phys. Fluids B* **4**, 2203 (1992).

²⁷See AIP Document No. PAPS PFBPE-05-2698-3 for 3 pages of J. J. Barnard, H. D. Shay, S. S. Yu, A. Friedman, D. P. Grote, *1992 Linear Accelerator Conference Proceedings*, 24–28 August 1992, Ottawa, Ontario, Canada, edited by C. R. Hoffman (Scientific Document Distribution Office, AECL, Chalk River, Ontario, Canada, 1992), Vol. 1, p. 229. Order of PAPS number and journal reference from American Institute of Physics, Physics Auxiliary Publication Service, 335 East 45th Street, New York, NY 10017. The price is \$1.50 for each microfiche (60 pages) or \$5.00 for photocopies of up to 30 pages, and \$0.15 for each additional page over 30 pages. Airmail additional. Make checks payable to the American Institute of Physics.

²⁸E. P. Lee, *Part. Accel.* **37-38**, 307 (1992).

²⁹J. F. DeFord and G. D. Craig, *Part. Accel.* **37-38**, 111 (1992).